Available online at www.sciencedirect.com

ScienceDirect

Procedia Computer Science 00 (2014) 000–000

Procedia Computer Science

www.elsevier.com/locate/procedia

6th International conference on Intelligent Human Computer Interaction, IHCI 2014

Assistive Driving Simulator with Haptic Manipulator Using Model Predictive Control and Admittance Control

Masashi Yamashita[*a]

[*a] *Toyota Technological Institute*
Hisakata 2-12-1, Tempaku-ku, Nagoya, Aichi, 468-8511 Japan

Abstract

In this paper, we propose an assistive driving simulator with a haptic manipulator for training older drivers. In the training process, it is desirable to limit the tracking error. A haptic device's input power can be adjusted to ensure safety and learning. Using model predictive control, we consider the above limitations as constraints and design controllers to minimize the costs in real time. In addition to good maneuverability, an admittance control is applied to realize an adequate reaction force. Based on experimental results, the designed model predictive controller, combined with the admittance controller, achieves excellent tracking performance in both an autonomous mode and assistive mode.

Peer-review under responsibility of the Scientific Committee of IHCI 2014.

Keywords: model predictive control; driving simulator; haptic manipulator, admittance control

1. INTRODUCTION

As society ages, the number of drivers older than 65 continues to increase worldwide. According to the National Highway Traffic Safety Administration in the United States, an average of 500 older adults are injured every day in automobile accidents[1]. Exercising regularly using a driving simulator is a useful way to maintain and increase an older adult's driving abilities. In many driving simulators, there is a steering device with a servomotor to generate a road reaction force. However, there is no haptic device to guide a driver in the correct maneuver while performing lane keeping on a curve. On the other hand, an assistive robot with haptic guidance has been used in a rehabilitation training procedure and demonstrated high reproducibility and good quantification[2]. The final goal in this study is to realize an assistive driving simulator with a haptic device to allow older adult drivers to maintain good driving abilities. Considering the training procedure for a driver, it is desirable to adjust a haptic device's input power to a

* Corresponding author. Tel.: +81-52-809-1813 .
E-mail address: m-yamashita@toyota-ti.ac.jp .

Peer-review under responsibility of the Scientific Committee of IHCI 2014.

suitable value, according to the driver's status. A hard assistive force is adequate in an initial stage, whereas it is better to decrease this assistive force in accord with the training procedure. This concept is analogous to a rehabilitation training procedure. The adjustment of the control parameters is also an important issue, and the efficacy of such adjustments has been evaluated[3]. In addition to the need for safety, it is important to have the ability to stay in a lane.

In this paper, we propose an assistive driving simulator with a haptic manipulator that uses model predictive control theory. Model predictive control involves a design methodology that solves optimal control problems in real time, making it possible to predict state variables by using a model, and minimizes the cost function with constraints [4, 5]. The terms for the cost function include the tracking error between the lane and the driving vehicle and the input power of the haptic device. In addition, considering the constraints for these terms enables us to realize an adequate training procedure and safety guidance, as mentioned above. In the design process, Laguerre functions are used to reduce the controllers' calculating costs. With regard to implementation, a state observer is designed to estimate the state variables of the augmented model. For good maneuverability, it is important to present a reactive force in proportion to the maneuvering force of a human subject using an admittance control. The admittance control is able to realize a desired virtual stiffness and damping for the haptic device. Because we use a PHANTOM Omni as a haptic device, no force sensor is needed to measure an external force such as the maneuvering force. In this study, a disturbance observer is utilized to estimate the external force. Because the assistive driving system was designed based on a complex mechanical model with constraints on the inputs and outputs, as well as the force-sensitive human dynamics, it is appropriate to consider both the model predictive controller and the admittance controller as basic components. The model predictive controller and admittance controller are evaluated in experimental tests using a CarSimDS driving simulator and the PHANTOM Omni haptic manipulator.

2. EXPERIMENTAL SETUP

Figure 1 shows the experimental setup of the assistive driving simulator. The PHANTOM Omni haptic device has six degrees of motion with three servomotors and six encoders[6]. When the stylus is fixed to the second arm of the Omni, we can use it as a mechanical robotic manipulator with three degrees of motion. For a driving simulator, we use the CarSimDS, which uses a vehicle model with twenty-seven degrees of freedom and is able to simulate the vehicle dynamics in real time[7]. In the driving training process, subjects use a grip attached to the second arm of the Omni that they manipulate while driving the vehicle and tracking the lane on the monitor. The control system consists of an admittance controller on the Omni's PC and a model predictive controller on the CarSimDS's PC. The steering angle that is generated by manipulating the grip of the Omni is sent to the CarSimDS's PC. After calculating the vehicle dynamics and model predictive control, the road reaction force and control command are sent to the Omni's PC. These signals are used for calculating the reaction force for the Omni. Note that the Omni does not have sensors to measure external forces such as human manipulating forces, and the CarSimDS has sensors to measure white lanes to calculate the error between the vehicle and the road for a position and pose.

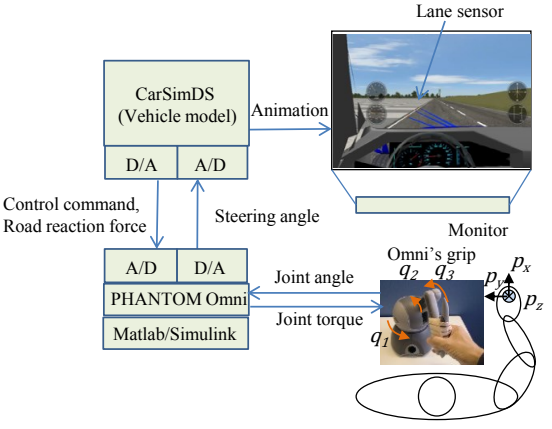

Fig. 1 Experimental setup

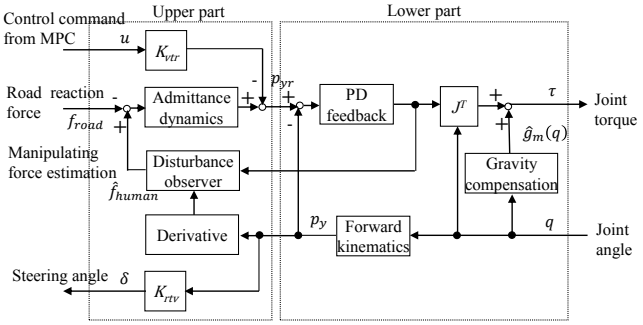

Fig. 2 Diagram of admittance controller (P_y axis)

3. CONTROL SYSTEM DESIGN

In this paper, two kinds of controllers are designed and implemented within the experimental setup: an admittance controller is designed to present a good reactive force to a human subject, and a model predictive controller with constraints is designed to minimize the tracking error of the vehicle and control commands for the haptic device.

3.1. Admittance Controller

In this paper, the admittance control law based on the positional control scheme is applied. Figure 2 shows a diagram of the controller. First, the mathematical model of the mechanical robotic device is derived as follows:

$$\tau = M_m(q)\ddot{q} + B_m\dot{q} + D_m(\dot{q}) + g_m(q) - J^T f_{ext} \quad (1)$$

where M_m is the moment of inertia, B_m is the viscous friction coefficient, D_m is the Coulomb friction term, g_m is the gravity term, and J^T is the transpose of the Jacobian matrix. The driving torque of the servomotor τ, the angle of the servomotor q at each joint $i = 1,2,3$, and the external force f_{ext} at the end effector, i.e., the grip, are defined as follows.

$$\tau = [\tau_1 \quad \tau_2 \quad \tau_3]^T \quad (2)$$

$$q = [q_1 \quad q_2 \quad q_3]^T \quad (3)$$

$$f_{ext} = [0 \quad f_{human} \quad 0]^T \quad (4)$$

where f_{human} is the manipulating force exerted by a human.

Assuming that the viscous friction and Coulomb friction are small, the lower part of the controller is designed as shown here:

$$\tau = -J^T\{K_p(p - p_{ref}) + K_d(\dot{p} - \dot{p}_{ref})\} + \hat{g}_m(q) \quad (5)$$

where K_p and K_d are the proportional and derivative gains of the PD controller, respectively, and $\hat{g}_m$ is the gravity compensation term.

The position p of the end effecter in the work space is calculated using the forward kinematics [8].

$$p = [p_x \quad p_y \quad p_z]^T = FK(q) \quad (6)$$

Here, *FK* is a function indicating the forward kinematics.

The reference p_{ref} of the positions is defined as follows.

$$p_{ref} = [0 \quad p_{yr} \quad 0]^T \quad (7)$$

For the upper part of the controller, the reference p_{yr} of the lateral position is derived using the external force and admittance dynamics:

$$p_{yr} = (sD_{adm} + K_{adm})^{-1}(f_{human} - f_{road}) - K_{vtr}u \quad (8)$$

where s is the Laplace operator; D_{adm} and K_{adm} are the damping and stiffness coefficients of the admittance control, respectively; f_{human} is the manipulating force; f_{road} is the road reaction force; K_{vtr} is the coefficient for translating from the vehicle to the robotic device; and u is the control input from the model predictive controller.

Because the Phantom Omni does not have a force sensor, a disturbance observer is used to estimate the manipulating force.

$$\hat{f}_{human} = (T_{do}s + 1)^{-1}s(M_y\dot{p}_y) + (T_{do}s + 1)^{-1}f_{cy} \quad (9)$$

where $\hat{f}_{human}$ is the manipulating force estimation, T_{do} is the time constant of the disturbance observer, M_y is the inertia of the Omni on the p_y axis, and f_{cy} is the control force on the p_y axis.

$$f_{cy} = K_p(p_y - p_{yr}) + K_d(\dot{p}_y - \dot{p}_{yr}) \quad (10)$$

Figure 3 shows the experimental performance of the disturbance observer. The dotted and solid lines indicate measurements by a force sensor and the estimations of the observer, respectively. The findings in this figure confirm that a good estimation was realized. Note that this force sensor was added only to confirm the estimation performance. Figure 4 shows the experimental performance of the admittance controller. This figure confirms that the desired stiffness and damping were achieved.

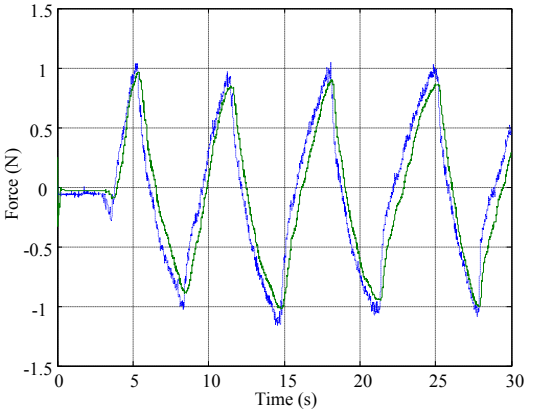

Fig. 3 Performance of disturbance observer

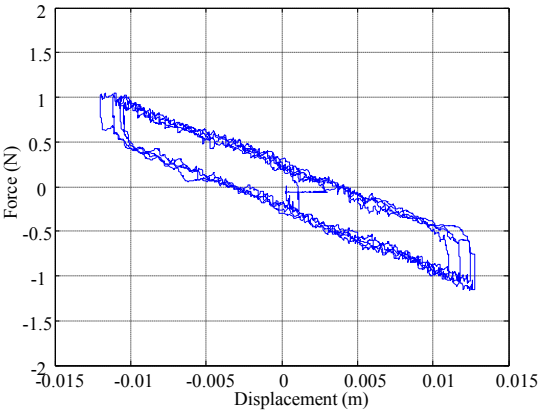

Fig. 4 Performance of admittance controller

3.2. Formulation of Model Predictive Control

In this paper, a bicycle model is considered to design a model predictive controller. Figure 5 shows the coordinate systems. The X and Y are global coordinates, and the X_v and Y_v are the coordinates of the vehicle. In this figure, ψ is the yaw angle, L_{ah} is the look-ahead distance, c_r is the road curvature, e_y is the lateral error between the desired path and the vehicle's position, and e_h is the heading error between the path and the vehicle's pose.

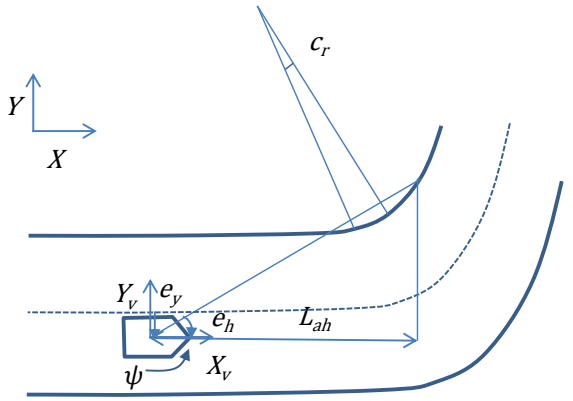

Fig. 5 Coordinate systems

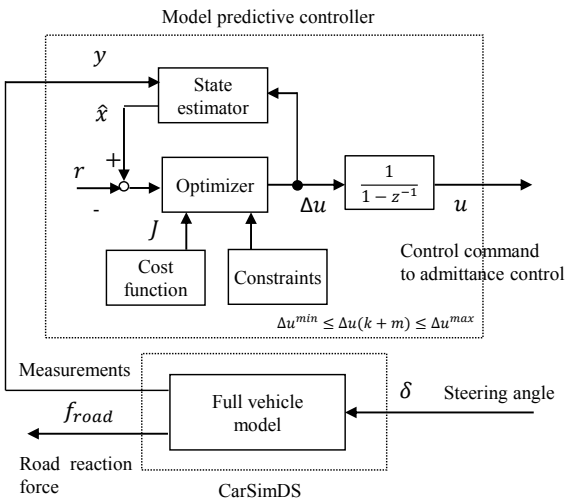

Fig. 6 Diagram of model predictive controller

When we assume that the longitudinal velocity v_x of the vehicle is constant, the lateral and yaw motions can be described as a linear time invariant system. By including the road curvature in the vehicle model, state space equations can be derived as follows:

$$\dot{x}_m = A_v x_m + B_{1v}\delta + B_{2v}c_r \quad (11)$$

$$y = C_v x_m + D_{1v}\delta + D_{2v}c_r \quad (12)$$

where δ is the steering angle, $x_m = [v_y \quad \dot{\psi} \quad e_y \quad e_h]^T$ is the state variable, v_y is the lateral velocity of the vehicle, and $y = [e_y \quad e_h]^T$ is the measurement. The matrices of the state space model are as follows[8].

$$A_v = \begin{bmatrix} a_1 & a_2 & 0 & 0 \\ a_3 & a_4 & 0 & 0 \\ -1 & 0 & 0 & v_x \\ 0 & -1 & 0 & 0 \end{bmatrix}, B_{1v} = \begin{bmatrix} b_1 \\ b_2 \\ 0 \\ 0 \end{bmatrix}, B_{2v} = \begin{bmatrix} 0 \\ 0 \\ -L_{ah} v_x \\ v_x \end{bmatrix}$$

$$C_v = \begin{bmatrix} 0 & 0 & 1 & 0 \\ 0 & 0 & 0 & 1 \end{bmatrix}, D_{1v} = \begin{bmatrix} 0 \\ 0 \end{bmatrix}, D_{2v} = \begin{bmatrix} 0 \\ 0 \end{bmatrix}$$

Elements in the state space model are shown in the Appendix.

To apply a discrete-time model predictive control, the continuous state space model is discretized. The sampling time is 0.0025 (s).

$$x_m(k+1) = A_m x_m(k) + B_m u(k) \tag{13}$$

$$y(k+1) = C_m x_m(k) \tag{14}$$

Here, u is the control input, i.e., the control command to δ, A_m, B_m, and C_m are the matrices of the discrete state space model, and k is the time instant.

Using the increments of the state variables and the control input to design the model predictive controller is convenient. Therefore, the above state space model is transformed into the following augmented model:

$$x(k+1) = Ax(k) + B\Delta u(k) \tag{15}$$

$$y(k+1) = Cx(k) \tag{16}$$

where the incremental difference in the state variables, the incremental difference in the control input, and the matrices of the augmented model are as described below.

$$x(k) = [\Delta x_m(k)^T \quad y(k)]^T, \Delta x_m(k) = x_m(k) - x_m(k-1), \ \Delta u(k) = u(k) - u(k-1)$$

$$A = \begin{bmatrix} A_m & 0_m \\ C_m A_m & 1 \end{bmatrix}, B = \begin{bmatrix} B_m \\ C_m B_m \end{bmatrix}, C = \begin{bmatrix} 0_m & 1 & 0 \\ 0_m & 0 & 1 \end{bmatrix}$$

3.3. Model Predictive Controller

We first designed the model predictive controller without constraints by using Laguerre functions, as described in a previous study[9]. Because Laguerre functions are able to represent the model dynamics using a few parameters, this function can be very effective at reducing the calculation costs.

In this study, the cost function is defined as follows:

$$J = \sum_{m=1}^{N_p} \big(r(k) - y(k+m|k)\big)^T Q_w \big(r(k) - y(k+m|k)\big) + \sum_{m=0}^{N_c-1} (\Delta u(k+m))^T r_w (\Delta u(k+m)) \tag{17}$$

where $y(k+m|k)$ are the predicted output variables for instant m calculated at time instant k, $\Delta u(k+m)$ is the future control movement for instant m, N_p is the prediction horizon, N_c is the control horizon, and Q_w *and* r_w are the weights for tuning the closed loop performance. The first term has the objective of minimizing the tracking errors between the predicted output and the reference signal, while the second term has the objective of restricting the input energy for control.

In the case of no constraints, the model predictive controller is derived in the form of a state feedback control.

$$\Delta \mathrm{u(k)} = -L(0)^T \Omega^{-1} \Psi (x(k) - R(k)) \tag{18}$$

where $L(0)$ and a are the initial condition and pole of the Laguerre network, respectively.

$$\Omega = \sum_{m=1}^{N_p} \phi(m) C^T Q_w C \phi(m)^T + r_w \tag{19}$$

$$\Psi = \sum_{m=1}^{N_p} \phi(m) C^T Q_w C A^m \tag{20}$$

$$\phi(m)^T = \sum_{i=0}^{m-1} A^{m-i-1} B L(i)^T \tag{21}$$

$$R(k) = [0 \quad 0 \quad 0 \quad 0 \quad r(k)]^T \tag{22}$$

In this study, $r(k) = [0 \quad 0]^T$ is desired.

Considering the hard constraints in controller design problems requires real-time optimization. The active set method is adopted to solve the quadratic programming problem. In this optimization, the incremental difference in the control input is represented by the Laguerre function as follows:

$$\Delta u(k+m) = L(m)^T \eta \tag{23}$$

Using (19), (20), and (23), the cost function is represented in the matrix form:

$$J = \eta^T \Omega \eta + 2\eta^T \Psi x(k) \tag{24}$$

In this paper, we consider the constraints on the difference and amplitude of the control input and the output for the lateral error, to strictly restrict the input and output power:

$$\Delta u^{min} \le \Delta u(k+m) \le \Delta u^{max} \tag{25}$$

$$u^{min} \le \sum_{i=0}^{m-1} \Delta u(k+i) + u(k-1) \le u^{max} \tag{26}$$

$$y^{min} \le CAx(k) + CBL(0)^T \eta \le y^{max} \tag{27}$$

Finally, by applying the active set methods shown previously [(24), (25), (26), and (27)] and solving the quadratic programming problem at every sampling, the model predictive controller with constraints is obtained in the form shown (23) with $m = 0$.

To estimate the state variables, the observer is designed and implemented as a state estimator as follows:

$$\hat{x}(k+1) = A\hat{x}(k) + B\Delta u(k) + K_{ob}(y(k) - C\hat{x}(k)) \tag{28}$$

where $\hat{x}$ is the estimated state variable, and K_{ob} is the observer gain vector. The poles of the error system matrix $A - K_{ob}C$ are chosen to quickly satisfy the convergence to zero.

Figure 6 shows a diagram of the model predictive controller. This controller consists of the optimizer, cost function, constraints, and state estimator. The output of this controller is transmitted to the admittance controller as an external control command.

4. EXPERIMENTAL RESULTS

In this study, we used middle-aged drivers to evaluate the controllers designed in the previous section. This evaluation was planned as a preliminary test before training older drivers.

First, we evaluated the performance of the closed loop system with an autonomous mode. The autonomous mode means there was no manipulation by the subject, i.e., it was hands-free. Therefore, this performance mainly indicates the tracking performance by the model predictive controller.

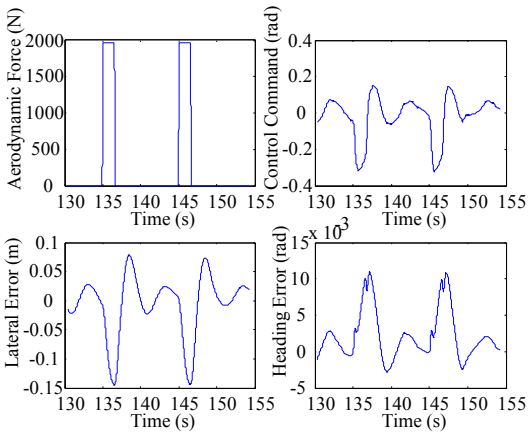

Fig. 7 Experimental results for autonomous mode while running at 70 km/h on straight course.

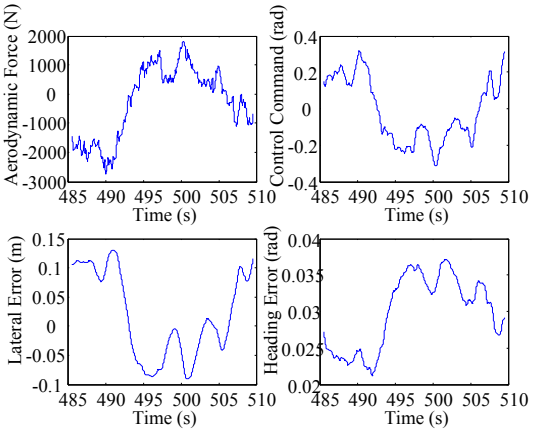

Fig. 8 Experimental results for autonomous mode while running at 70 km/h on R500 curve.

In the autonomous mode, the specification of the closed loop system is defined as follows:

$$|e_y| < 0.2\ (m)$$

$$\text{subject to } |\text{the lateral aerodynamic force}| < 3000(N),\ |\text{the road curvature}| < 0.002$$

Figures 7 and 8 show the experimental results of the autonomous mode tests while running at 70 km/h on the straight course and on the R500 curve, respectively. In the upper part of each figure, the left and right graphs show the aerodynamic force at the center of gravity in the lateral direction and the control command from the model predictive controller, respectively. In the lower part of each figure, the left and right graphs show the lateral error and heading error between the vehicle and the road, respectively. In spite of strong lateral winds such as pulses (see

Figure 7) and a continuous disturbance (see Figure 8), the performance for the lateral error was satisfied under the specification.

Next, we evaluate the performance of the model predictive control with constraints under an external force exerted by a subject. In this mode, the constraints to be confirmed are as follows:

$$y^{max} = 0.6\ (\mathrm{m}),\ y^{min} = -0.8(m),\ u^{max} = 2.1\ (\mathrm{rad}),\ u^{min} = -2.1\ (rad),$$
$$\Delta u^{max} = 0.5\ (\mathrm{rad}),\ \Delta u^{min} = -0.75\ (rad)$$

Figure 9 shows the experimental results of the model predictive control with constraints under the external force exerted by a subject while running at 70 km/h on the straight course. In the upper part of the figure, the left and right graphs show the manipulating force by the subject and the lateral error, respectively. In the lower part of the figure, the left and right graphs show the control command and incremental control command, respectively.

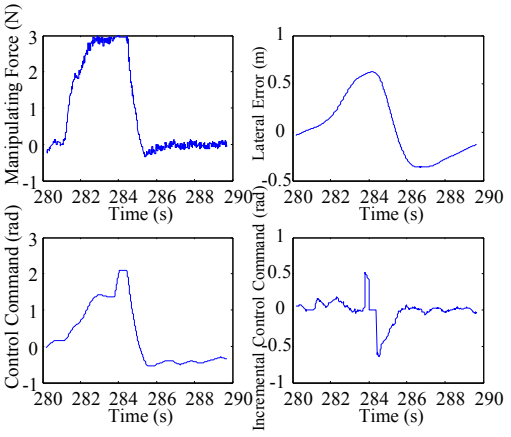

Fig. 9 Performance of model predictive control with constraints under manipulating force

The lateral error increases as the manipulating force increases. When the lateral error is greater than 0.6 (m) at 284 (s), the control command drastically increases and is limited to a value of 2.1 (rad). Because the limits of the incremental control command worked very well, it was confirmed that the model predictive control with constraints achieved the desired performance.

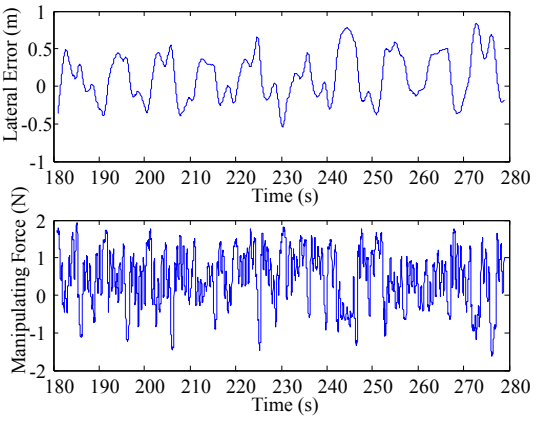

Fig. 10 Experimental results for manual mode

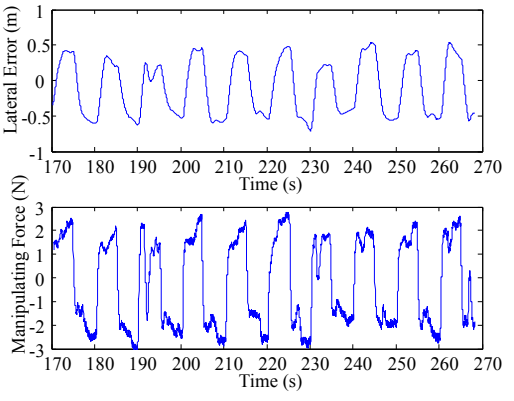

Fig. 11 Experimental results for assistive mode

Finally, we evaluate the performance of the closed loop system with an assistive mode. The assistive mode indicates that the subject is manipulating the grip of the Omni and tracking the white lane. Therefore, this performance indicates the tracking performance by both the model predictive controller and the human subject assisted by the admittance controller. In other words, the model predictive controller brings the lateral error equilibrium to zero, and the admittance controller helps the human subject to move the lateral error deviation to a

target using a linear reaction force. The above equilibrium represents an average signal, and the above deviation represents a difference from this average. In this test, the equilibrium and deviation of the lateral error were evaluated. Figures 10 and 11 show the experimental results of the manual and assistive mode tests while running on the straight course at 70 km/h under the above continuous lateral wind and executing the lateral movement from -0.5 (m) to 0.5 (m), respectively. The upper and lower parts of each figure show the lateral error and manipulating force, respectively. In the manual mode, the equilibrium of the lateral error moves slightly up in the positive direction, and the deviation is unstable around 0.5 (m) and -0.5 (m). In the assistive mode, the equilibrium remains around zero, and the deviation shows good reproducibility around 0.5 (m) and -0.5 (m). A comparison of the lower parts of Figure 10 with Figure 11 shows that the stable manipulating force assisted by the admittance controller makes it possible to easily execute a tracking performance.

5. CONCLUSIONS

In this paper, we proposed an assistive driving simulator with a haptic manipulator for training older drivers. In the training process, it is desirable to limit the tracking error. A haptic device's input power can be adjusted to ensure safety and learning. Using model predictive control, we considered the above limitation constraints and designed controllers to minimize the costs in real time. In addition to good maneuverability, an admittance control was applied to realize an adequate reaction force. Based on the experimental results, the designed model predictive controller, combined with the admittance controller, achieved excellent tracking performance in both an autonomous mode and an assistive mode. Further research will consider practical evaluations of the training of older adult drivers. In addition, it is expected that age-related decreases in cognitive function could be reduced by such training.

Acknowledgment

This work was supported by JSPS KAKENHI Grant Number 25330247.

Appendix

Elements in the state space model can be derived as follows:

$$a_1 = -(C_f + C_r)/(M_v v_x),\ a_2 = -v_x - (C_f L_f - C_r L_r)/(M_v v_x),\ a_3 = -(C_f L_f - C_r L_r)/(I_z v_x)$$
$$a_4 = -(C_f {L_f}^2 + C_r {L_r}^2)/(I_z v_x),\ b_1 = \left(C_f K_{sg}\right)/M_v,\ b_2 = (C_f L_f K_{sg})/I_z$$

where C_f is the cornering stiffness of the front tire, C_r is the cornering stiffness of the rear tire, M_v is the vehicle mass, L_f is the distance between the front axle and the center of gravity of the vehicle, L_r is the distance between the rear axle and the center of gravity of the vehicle, I_z is the moment of inertia for yaw motion, and K_{sg} is the gear ratio between the front wheel angle and the steering angle.

References

1. National Highway Traffic Safety Administration. Traffic Safety Facts :Older Population. DOT HS 811161; 2008.
2. Hogan N, Aise ML, Volpe BT. Robot-Aided Neurorehabilitation. IEEE Trans. On Rehabilitation Engineering; 1998. vol.6, no.1, p.75-87.
3. Riener R, Lunenburger L, Jezernik S, Anderschitz JM, Colombo G, Dietz V. Patient-cooperative strategies for robot-aided treadmill training: first experimental results. IEEE Trans Neural Syst Rehabil Eng.; 2005. 13(3), p.380-394.
4. Garcia CE, Prett DM, Morari M. Model predictive control: theory and practice-a survey. Automatica; 1989. vol. 25, p.335-348.
5. Rawlings JB. Tutorial overview of model predictive control. IEEE Control System Magazine; 2000. vol. 20, p. 38-52.
6. Silva A. PHANTOM Omni Haptic Device: Kinematic and Manipulability. Electronic, Robotics and Automotive Mechanics Conference; 2009. CERMA '09, p. 193-198.
7. Sayers MW. Symbolic Vector/Dyadic Multibody Formalism for Tree-Topology Systems. Journal of Guidance, Control, and Dynamics; 1991. vol.14, No. 6, p.1240-1250.
8. Cerones V, Chinu A, Regruto D. Experimental Results in Vision-based Lane Keeping for Highway Vehicles. Proc. American Control Conference, Anchorage, Alaska; 2002.
9. Wang L. Model Predictive Control System Design and Implementation using MATLAB. Springer-Verlag; 2009.